CF-LIBS quantification and depth profile analysis of Be coating mixed layers

Dwivedi, V.; Marín-Roldán, A.; Karhunen, J.; Paris, P.; Jõgi, I.; Porosnicu, C.; Lungu, C. P.; van der Meiden, H.; Hakola, Antti; Veis, P.

Published in:
Nuclear Materials and Energy

DOI:
10.1016/j.nme.2021.100990

Published: 01/06/2021

Document Version
Publisher's final version

Nuclear Materials and Energy 27 (2021) 100990

Contents lists available at ScienceDirect

Nuclear Materials and Energy

journal homepage: www.elsevier.com/locate/nme

CF-LIBS quantification and depth profile analysis of Be coating mixed layers

V. Dwivedi [a], A. Marín-Roldán [a], J. Karhunen [b], P. Paris [c], I. Jõgi [c], C. Porosnicu [d], C.P. Lungu [d], H. van der Meiden [e], A. Hakola [f], P. Veis [a,*]

[a] DEP, FMPI, Comenius University, Mlynská dolina F2, 842 48 Bratislava, Slovakia
[b] Aalto University, Dept. of Applied Physics, P.O. Box 11100, 00076 Aalto, Finland
[c] Institute of Physics, University of Tartu, W. Ostwaldi 1, 50411 Tartu, Estonia
[d] INFLPR 409, Magurele, Jud Ilfov 077125, Bucharest, Romania
[e] DIFFER, De Zaale 20, NL-5612 AJ Eindhoven, Netherlands
[f] VTT, P.O. Box 1000, 02044 VTT, Finland

ARTICLE INFO

Keywords:
Be-coated samples
Fuel retention
Depth profile
Quantification
CF-LIBS

ABSTRACT

A remote LIBS system is being considered as an analysis tool in ITER for monitoring the erosion and fuel retention in the first wall. This necessitates further investigation of the performance of LIBS for thick co-deposited layers consisting of ITER-relevant materials. The main goal of this work is determining the fuel content of the samples and D depth profile by LIBS and to compare the results with those obtained by other methods. The studied samples were Be-based mixed coatings on W substrates, containing D and in some cases C, O, or both. These impurities are relevant not only for ITER, but also for other fusion devices, such as JET-ILW. The laser ablation was performed at 10 mbar Ar pressure using a 5 ns pulse Nd:YAG laser at 1064 nm. Suitable Be and Ar spectral lines were employed for the evaluation of the electron temperature of the plasma using multi-elemental Saha-Boltzmann (MESB) plots. The electron density was obtained from the Stark broadening of the D_α and H_α spectral lines following deconvolution. The average elemental content of each coating was then obtained by calibration-free LIBS (CF-LIBS) and are in agreement with other techniques (TOF–ERDA, IBA).

1. Introduction

Understanding and controlling the interaction between plasma and plasma-facing materials (PFMs) is required to realize high performance in fusion devices. The PFM in the ITER main chamber will be Be. Its erosion and subsequent migration in the edge plasma will lead to the formation of co-deposited layers with fuel and impurities [1–5]. During tokamak operation, the structure, composition, roughness, thickness, etc., of the PFMs may vary, all altering fuel retention [6–9] and especially the newly deposited layers can trap a significant fraction of the plasma fuel [10]. Thus, it is crucial to monitor *in situ* the composition of these layers by LIBS [11]. The depth profile analysis of fusion-relevant bulk materials and deposited layers has been intensively studied by LIBS [12–21], as it has been proven to fulfill all the requirements for an online analysis, in vacuum and remotely for the next nuclear fusion device in ITER. The fuel retention has also been extensively studied by LIBS [13,22–24] but usually without the quantification approach.

The quantification of the elements by LIBS requires either extensive calibration procedures or the application of Calibration Free (CF) LIBS. The CF-LIBS approach allows quantifying each element present in the sample without the need of calibration references of known composition and fuel content. CF-LIBS allows obtaining quantitative information by taking into account the physical parameters that characterize the plasma conditions: the electron density (n_e) and temperature (T_e). The n_e is usually determined by the Stark broadening of the Balmer-α line of hydrogen at around 656 nm, while the T_e is evaluated by the Saha-Boltzmann plot (1/slope) [25].

As the CF–LIBS approach is very sensitive to the T_e and n_e values, several conditions are necessary for a suitable Saha-Boltzmann plot: among others [26], presence of at least two different degrees of ionization, the widest range of higher possible energies (with as many spectral lines as possible for each degree of ionization), sufficient precision of the Einstein coefficients. Thus, one of the main conditions for precise T_e evaluation, is to have at least one element with a large energy gap with sufficient precision of the Boltzmann data points related to the spectral lines. CF-LIBS has shown promising results in the analysis of various fusion-relevant materials [15,21,27,28].

The aim of this work is determining D retention and its depth profile

* Corresponding author.
E-mail address: pavel.veis@fmph.uniba.sk (P. Veis).

https://doi.org/10.1016/j.nme.2021.100990
Received 30 July 2020; Received in revised form 11 March 2021; Accepted 25 March 2021
Available online 1 April 2021

of Be-based mixed coatings with small additions of light elements (C, O, H) and retained fuel (D) by CF-LIBS, similarly to the analyses in our previous paper [27] where we studied for the first time D retention in BeW mixed layer samples. The Be-based samples containing O and D will be representative for the deposits predicted for the first wall of ITER while the inclusion of C in the mixture would make the layers mimic those already observed on JET ILW (the PFMs for the initial phase of ITER operation are Be and W). LIBS measurements of six different samples were done in a collaboration between VTT Technical Research Centre of Finland, the Comenius University and the University of Tartu.

2. Materials and methods

2.1. Samples

The samples with mixed coatings of Be, O, C, and D in different ratios and thickness (5–15 μm) were deposited on a tungsten substrate at the National Institute for Laser, Plasma, and Radiation Physics in Romania, by high-power impulse magnetron sputtering in a high vacuum chamber [29]. The information regarding the measured samples can be seen in Table 1.

2.2. Analysis method

LIBS measurements of the above-mentioned samples were performed in a specially designed set-up in the Be-handling premises of VTT. A detailed description of the experimental set-up is reported elsewhere [12,15]. In brief, a Q-switched Nd:YAG laser (Brilliant B, Quantel) with its optical emission at 1064 nm with a pulse duration of 5 ns was used as a source to generate the plasma plume on the target material. The characteristic emission was collected by the acquisition optics (off-axis parabolic mirror and optical fiber bundle containing 50 fibers with diameters of 50 μm) connected to the spectrograph (Andor SR-750). This spectrograph is coupled with an Andor iStar 340 T camera. The laser fluence was kept low (4.5 J cm^{-2}) to obtain a low ablation rate with a stable plasma ignition.

The LIBS spectra were measured in 10 different pre-selected spectral ranges centered at 235, 275, 320, 365, 435, 475, 510, 642, 767, 844 nm, respectively, using a grating with 600 grooves/mm blazed at 500 nm, providing 40 nm wide spectral windows. For recording the Balmer-alpha lines of hydrogen isotopes at around 656 nm, a special grating with 1350 grooves/mm and blaze at 675 nm was used. The spectral resolution of the applied spectrometer with this grating was approximately 0.1 nm (experimentally verified by recording the HeNe laser line at 632.8 nm scattered from the diffuser). This configuration with a spectral window of 20 nm enabled partly resolving D_α and H_α lines. In order to enhance the signal to noise ratio by enhancing the collisional excitation and to improve the detectability and separation of the D_α and H_α lines, the LIBS measurements were performed at 10 mbar Ar background pressure. Considering the emission of both ions and neutrals, and the best signal to noise ratio, most of the measurements were performed with the gate delay time of 300 ns while the gate width was set to 500 ns. For easier separation of D_α and H_α lines, the measurements with higher resolution grating were made at a 2500 ns delay time and 2000 ns width gate. For each measurement spot on the sample, 50–100 laser pulses (upper limit for the thickest sample) were applied to determine the elemental depth profiles of the coating and reach the W substrate. The emitted plasma light was collected by a 50 optical fibers bundle (0.125 nm diameter) transformed from round to linear in the lateral direction of the sample surface. The spectral response curve of the entire optical system was evaluated using a deuterium-halogen calibration lamp (Ocean Optics DH-2000-cal). For the wavelengths above 400 nm, high passband filters with a transmittance of 90% were used in the desired spectral range to avoid the simultaneous detection of the second-order lines from lower wavelength ranges. All the measured spectra were corrected to the spectral response curve and the transmittance of the filter.

Table 1
Elemental composition and thickness of the measured Be-based samples. 100 °C refers to the temperature during the production process of sample 4. Samples 1–3 were produced at room temperature.

Sample	Elements	Thickness
1	BeOCD	5.7 μm
2	BeOD	11.1 μm
3	BeD	5.8 μm
4	BeOCD (100 °C)	12.0 μm

3. Results

Elemental LIBS depth profiles were extracted using persistent and representative lines. Examples of such profiles for samples 1 and 2 (see Table 1), using delay time of 300 ns, are shown in Fig. 1 together with corresponding depth profiles measured using secondary ion mass spectrometry (SIMS). Sample 2 is thicker than sample 1, as evidenced by W lines starting to appear some 8 laser pulses later in the LIBS profiles (see Fig. 1A and C) and proved by depth measurements of the SIMS craters using a stylus profilometer. The spectral lines applied for the depth profile are Be I 332.11 nm, 381.34 nm, 457.26 nm; H + D 656.28 nm; C I 247.85 nm; O I 777 nm, 844 nm; and W I 400.87 nm, 429.46 nm. Depth calibration was done by measuring the depths of the produced laser- or ion-beam craters by a stylus profilometer.

As it can be observed in Fig. 1(B and D), the SIMS results are in agreement with the LIBS depth profile analysis even if the signal ratios by LIBS and SIMS (e.g., for D/Be) are different since the yield of atoms and ions vary. A small bump can be observed for H + D in the interface layer-between sample 1 and substrate in Fig. 1(A) that is not observable in Fig. 1(B). Several factors can contribute to the occurrence of this bump, e.g., laser heating and diffusion of species, matrix effects, contamination of the interface between the Be-based layer and the substrate (e.g., due to water), as well as imperfections in the properties of the particular sample selected as an example in Fig. 1(A). Interestingly no such bumps can be seen in Fig. 1 (C), indicating that no single factor alone can explain the details of the depth profiles, but a thorough survey of the thermal, structural, and surface properties of the studied samples is required; this is beyond the scope of the present work. In this case, the presence of H could be caused by water contamination in the sample.

In all the measured spectra, a set of interference and self-absorption free lines was selected by comparing the measured data with simulated spectral lines [30]. Suitable Ar and Be spectral lines have been used for the evaluation of the electron temperature of the plasma using a Saha-Boltzmann plot, and for the final precise evaluation of the temperature, the multi-elemental Saha-Boltzmann plot of the neutral and ionic lines of both elements was used. Lines of other elements were not too numerous (other observed lines were C I line at 247.8 nm, O I lines at 777.5 nm and 844.6 nm, and H I-D I at 656.1 nm and 656.3 nm, respectively) for the temperature evaluation. For each sample, the line intensities were averaged (see table 2) over the range of laser shots where the intensities remained practically same according to LIBS depth profiles.

Fig. 2 shows (A) the multi-elemental Saha-Boltzmann (MESB) plot for Be I-II and Ar I-II, and (B) the Boltzmann plot (BP) of the selected emission lines of Be I-II, O I, C I, and H/D lines, in both cases for an averaged spectrum. The n_e has been determined by the Stark broadening of the Balmer α line of hydrogen at around 656 nm, while the T_e has been evaluated by the Saha-Boltzmann plot. The experimentally determined electron temperatures and densities are presented in Table 2.

Fig. 3(A) shows the resolved spectral lines belonging to D_α and H_α. This spectrum was obtained at longer delay time of 2500 ns to obtain narrower lines and therefore facilitate the deconvolution process and determination of the D/H ratio. According to Fig. 3, the experimental spectra are partially resolved, showing two peaks that consist of the

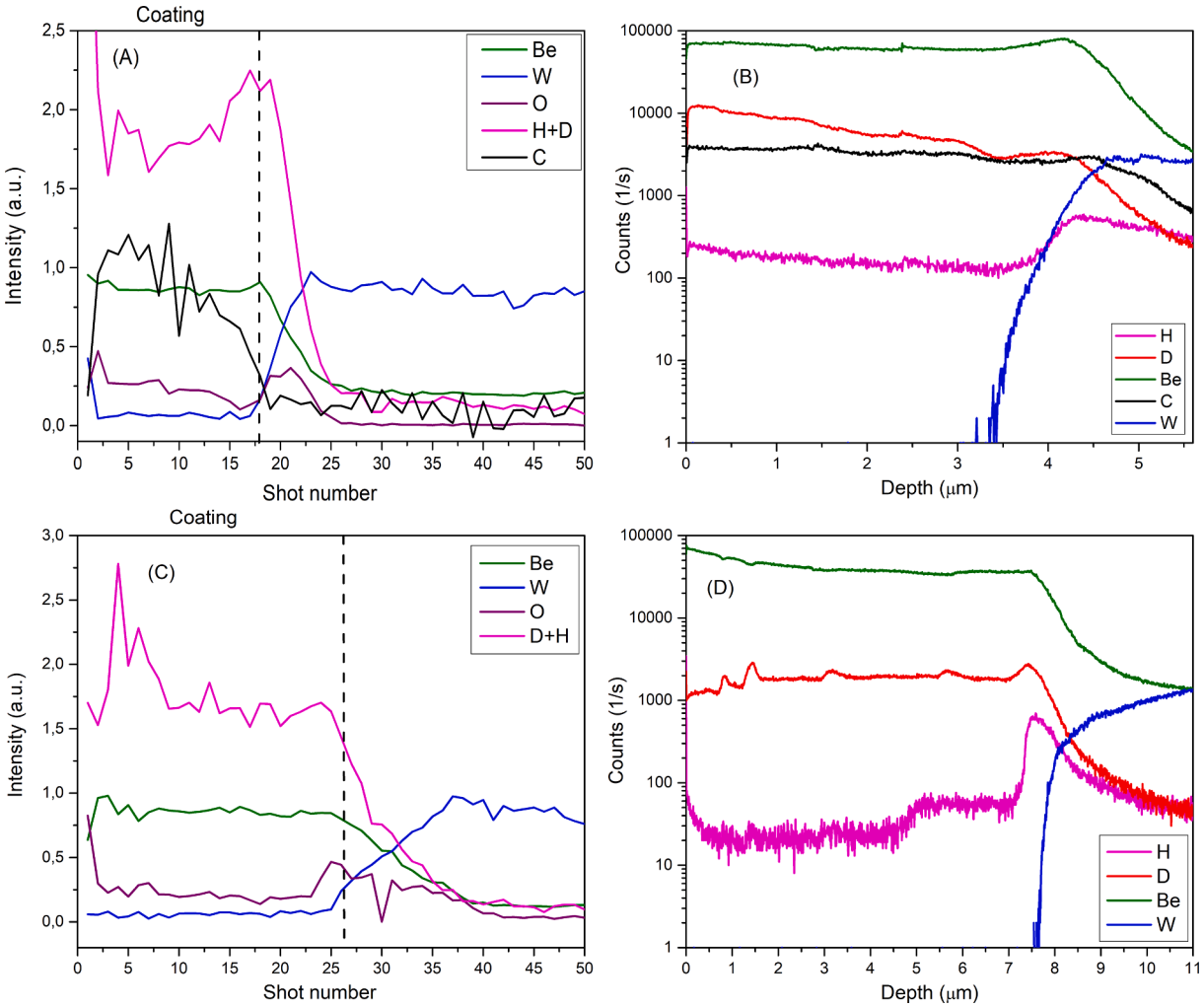

Fig. 1. (A, C) LIBS and (B, D) SIMS depth profiles of different elements (H, D, Be, C, O and W) in sample 1 (A, B) and sample 2 (C, D).

Table 2
Electron temperature, electron density, and ablation rate values.

Sample	Averaged spectra	T_e (eV)	$n_e \cdot 10^{16}$ (cm^{-3})	Ablation rate (nm/shot)
1	4–18	1.12 ± 0.02	3.80 ± 0.15	280
2	5–25	1.09 ± 0.02	3.17 ± 0.70	230
3	4–15	1.08 ± 0.02	3.40 ± 0.10	250
4	3–25	1.07 ± 0.02	3.80 ± 0.25	360

abovementioned spectral lines. To this end, a Lorentzian contour for the D_α (magenta line) and H_α (red line) with varying FWHM values have been used in the fitting procedure. Lorentzian contour resulted in a reasonably good fit of the experimental data even though the Gaussian component caused by the apparatus function (0.1 nm) was comparable with the Lorentzian component caused by the Stark broadening at 2500 ns. At 300 ns, the FWHM values were much higher (0.4–0.5 nm), and the Gaussian component had even smaller influence on the fitting. Nevertheless, the Gaussian component caused by the apparatus function and the Doppler broadening were considered in the determination of the electron density from the experimentally determined FWHM value. Fig. 3(B) shows the detailed depth profile for D_α and H_α for the spectrum acquired at a longer delay time (2500 ns) than Fig. 1, after the deconvolution process of the spectral lines shown in Fig. 3(A).

CF-LIBS was applied to quantify the elemental composition of the coating in 4 principally different Be-coated samples (with and without C and O). For each coating, the CF-LIBS procedure used the D line intensities, which were averaged over a similar range of laser shots (those spectra that maintain a stable LIBS intensity in the depth profile as shown in Fig. 1(A and C)), as shown in Table 2 for the T_e determination. The results were compared with other existing techniques: Time-Of-Flight Elastic Recoil Detection Analysis (TOF-ERDA) and Ion Beam Analysis (IBA) [29]. The elemental content in percentages (%) for each sample is presented in Table 3. These results are generally in agreement with TOF-ERDA, IBA and TDS measurements from [29]. The approximate uncertainty levels for these other techniques are ~ 10%, while for LIBS, the uncertainty level is ~ 20%. Please also note that TOF-ERDA only considers the very surface layer (<100–300 nm), while just one laser shot ablates already the same amount of material (see ablation rate in Table 2). Thus, the results of TOF-ERDA are not completely comparable with LIBS and IBA.

CF-LIBS results are dependent on the accuracy of the determination of the electron temperature and density. The electron temperature value is influenced by shot-to-shot variabilities of the lines used to construct the Saha-Boltzmann plot, by the accuracy of the determination of the spectral sensitivity of the system and by the accuracy of the electron density determination [31]. Electron density, in turn, is influenced by the accuracy of the determination of the FWHM of the D_α and H_α lines. In Fig. 4(A), we can observe that for a variation of the electron density by

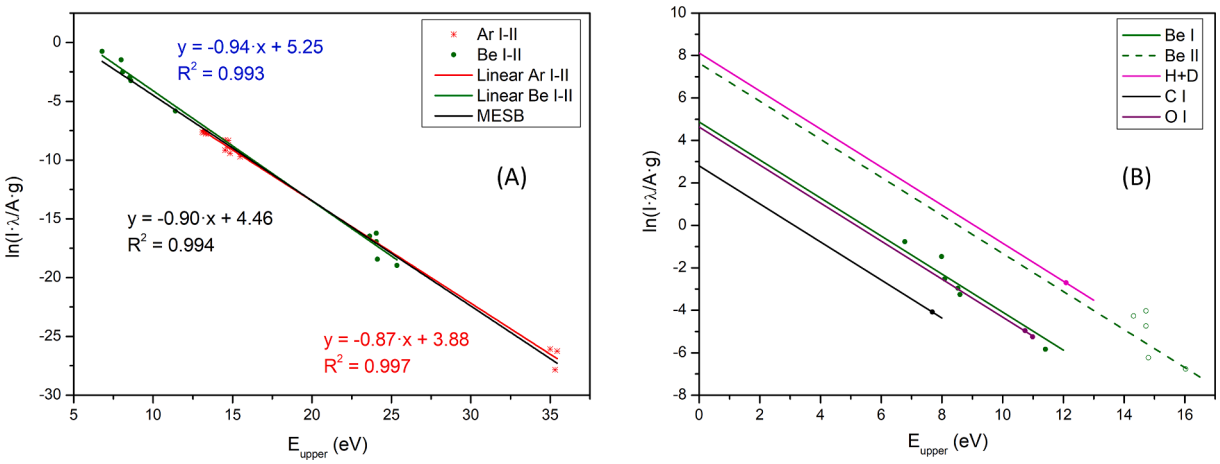

Fig. 2. (A) MESB plot for Be I and Ar I-II, (B) Boltzmann plot for Be I, O I, C I, and H/D spectral lines using the evaluated T_e from the MESB plot.

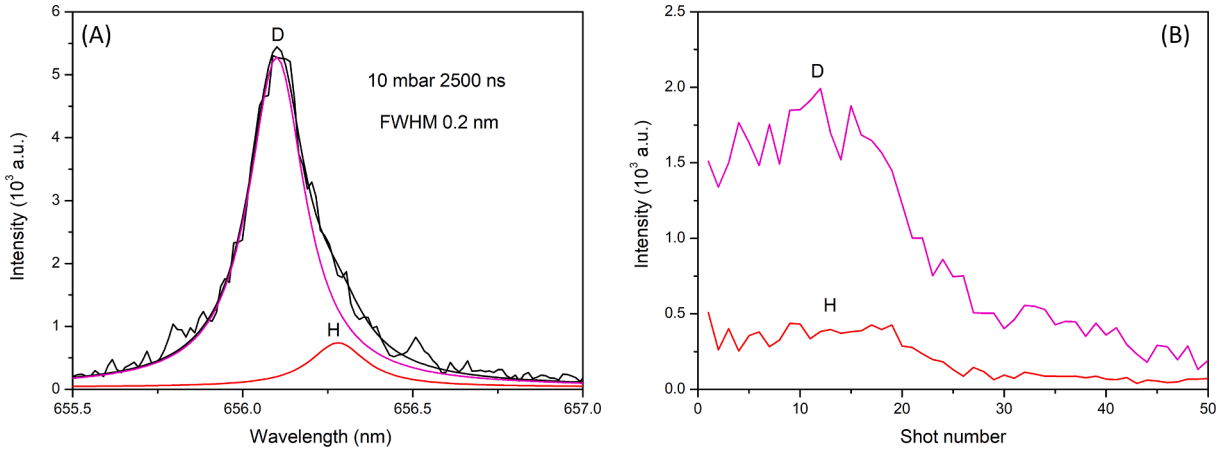

Fig. 3. (A) D_α and H_α spectral lines, spectrally resolved by Lorentz fittings at 656.1 nm and 656.3 nm, respectively, for the 8th laser shot of the sample 1; (B) Depth profiles of D and H intensities for the same sample.

Table 3
Atomic percentages for Be, O, C, H, and D.

Sample	Be%	O%			C%			H%	D%		
	LIBS	LIBS	TOF-ERDA	IBA	LIBS	TOF-ERDA	IBA	LIBS	LIBS	TOF-ERDA	IBA
1	52.1	7.6	4.0	12.0	5.0	8.0	11.0	8.4	26.9	44.0	38.0
2	54.0	8.0	3.1	0.0	—	0.3	—	13.6	24.4	26.0	24.6
3	60.9	5.5	0.9	—	—	0.1	—	14.6	19.0	20.0	19.0
4	55.4	8.2	2.8	7.5	1.1	6.1	5.0	8.2	27.1	23.0	4.5

1 order of magnitude, the percentage changes by ~ 50% for Be and ~ 35% for D. Thus, the uncertainty in the n_e evaluation for sample 1 changes the Be and D concentration by ~ 1.5 at.% and ~ 2 at.%, respectively. In Fig. 4(B), we can observe the variation in the Be composition in at% as a function of the T_e. From the regression formulas presented in the figure, we obtain the corresponding error in the Be and D concentration evaluation as ~ 18% and ~ 16%, respectively, due to the inaccuracy in the T_e evaluation of ± 0.02 eV. The global error in the LIBS concentration evaluation is, for the sample 1, 20 at.%. Similar values were also found for the other samples. Thus, the correct evaluation of the T_e is extremely important as it can strongly affect the value of the estimated elemental composition.

4. Conclusions

The depth profile analysis by LIBS and SIMS has been performed for 4 samples consisting of Be-based coatings. The quantification analysis for the composition of the samples (by averaging the spectra from the deposited layer) has been performed by CF-LIBS. The deconvolution of the H/D spectral line at 656 nm allowed to quantify H and D separately. It was found that D retention values measured by LIBS and reference methods (TOF-ERDA and IBA) correspond in general within 30% with each other. TOF-ERDA only considers the very surface layer (<100–300 nm), while LIBS measurements ablate the same amount of material within one laser shot, and several laser shots were averaged for the elemental composition analysis. The obtained concentration values for other elements obtained by LIBS are at least within a factor 2 in agreement with other techniques, except sample 4 (heat-treated sample up to 100 °C). In this case, the differences are higher: D deviated by a factor 6, and C by a factor 5 (Be was not compared, only LIBS data provided). These achievements show that LIBS is a reliable method for measuring retained fusion fuel as well as the composition of deposited layers in

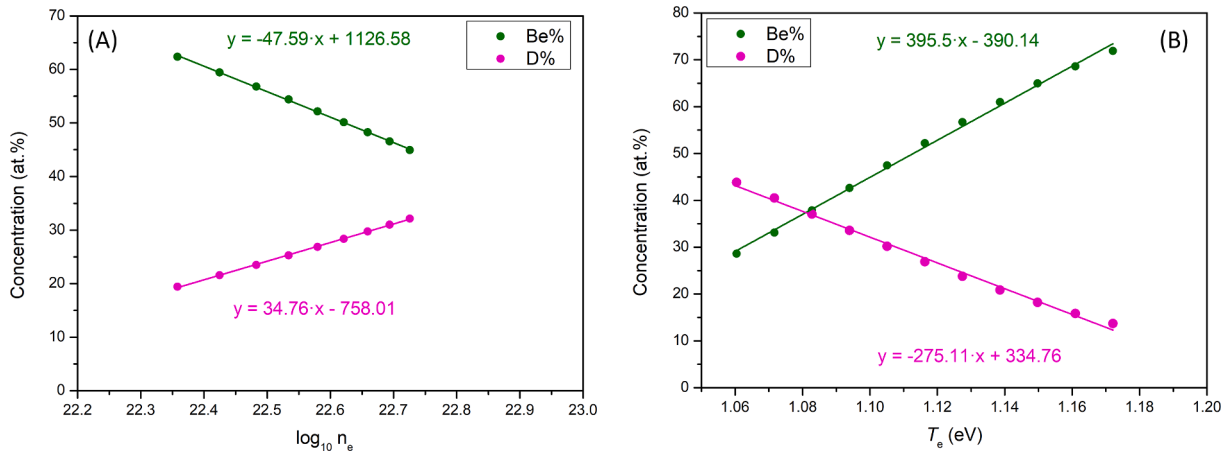

Fig. 4. (A) Variation in the at.% of the elemental composition when changing the n_e, (B) Variation in the at.% of the elemental composition when changing the T_e - case of the sample 1.

ITER and beyond.

Declaration of Competing Interest

The authors declare that they have no known competing financial interests or personal relationships that could have appeared to influence the work reported in this paper.

Acknowledgements

This work has been carried out within the framework of the EUROfusion Consortium and has received funding from the Euratom research and training programme 2014–2018 and 2019–2020 under grant agreement No.633053. The views and opinions expressed herein do not necessarily reflect those of the European Commission. Work performed under WP PFC. This work was also supported by the SRDA (APVV-16-0612) and by the VEGA (1/0903/17). VD would like to thank the Comenius University for the UK Young Grants (UK/64/2020_FMFI).

References

[1] S. Brezinsek, J.-E. Contributors, Plasma-surface interaction in the Be/W environment: conclusions drawn from the JET-ILW for ITER, J. Nucl. Mater. 463 (2015) 11–21.
[2] S. Brezinsek, J.E. Contributors, Fuel retention studies with the ITER-Like Wall in JET, Nucl. Fusion 53 (8) (2013) 083023, https://doi.org/10.1088/0029-5515/53/8/083023.
[3] M. Mayer, J.E.T. Contributors, Erosion and deposition in the JET divertor during the second ITER-like wall campaign, Phys. Scr. T170 (2017) 8.
[4] K. Heinola, J.E.T. Contributors, Experience on divertor fuel retention after two ITER-Like Wall campaigns, Phys. Scr. T170 (2017) 8.
[5] K. Heinola, J.E.T. Contributors, Long-term fuel retention and release in JET ITER-Like Wall at ITER-relevant baking temperatures, Nucl. Fusion 57 (8) (2017) 086024, https://doi.org/10.1088/1741-4326/aa747e.
[6] S. Almaviva, L. Caneve, F. Colao, R. Fantoni, G. Maddaluno, Remote-LIBS characterization of ITER-like plasma facing materials, J. Nucl. Mater. 421 (1-3) (2012) 73–79.
[7] R. Fantoni, S. Almaviva, L. Caneve, F. Colao, A.M. Popov, G. Maddaluno, Development of Calibration-Free Laser-Induced-Breakdown-Spectroscopy based techniques for deposited layers diagnostics on ITER-like tiles, Spectroc. Acta Pt. B-Atom. Spectr. 87 (2013) 153–160.
[8] A. Huber, B. Schweer, V. Philipps, N. Gierse, M. Zlobinski, S. Brezinsek, W. Biel, V. Kotov, R. Leyte-Gonzales, P.h. Mertens, U. Samm, Development of laser-based diagnostics for surface characterisation of wall components in fusion devices, Fusion Eng. Des. 86 (6-8) (2011) 1336–1340.
[9] S. Almaviva, L. Caneve, F. Colao, P. Gasior, M. Kubkowska, M. Łepek, G. Maddaluno, Double pulse Laser Induced Breakdown Spectroscopy measurements on ITER-like samples, Fusion Eng. Des. 96-97 (2015) 848–851.
[10] H. Roche, X. Courtois, P.h. Delaporte, T. Dittmar, D. Farcage, E. Gauthier, C. Hernandez, P. Languille, T. Loarer, L. Mercadier, M. Naiim Habib, J.-Y. Pascal, C. Pocheau, A. Semerok, E. Tsitrone, N. Vignal, C. Grisolia, Optimization of laser ablation technique for deposited layer removal on carbon plasma facing components, J. Nucl. Mater. 415 (1) (2011) S797–S800.
[11] G.S. Maurya, A. Marín-Roldán, P. Veis, A.K. Pathak, P. Sen, A review of the LIBS analysis for the plasma-facing components diagnostics, J. Nucl. Mater. 541 (2020), 152417.
[12] J. Karhunen, A. Hakola, J. Likonen, A. Lissovski, M. Laan, P. Paris, J. E. Contributors, Applicability of LIBS for in situ monitoring of deposition and retention on the ITER-like wall of JET - Comparison to SIMS, J. Nucl. Mater. 463 (2015) 931–935.
[13] M. Suchoňová, P. Veis, J. Karhunen, P. Paris, M. Pribula, K. Piip, M. Laan, C. Porosnicu, C. Lungu, A. Hakola, Determination of deuterium depth profiles in fusion-relevant wall materials by nanosecond LIBS, Nucl. Mater. Energy 12 (2017) 611–616.
[14] L. Mercadier, A. Semerok, P.A. Kizub, A.V. Leontyev, J. Hermann, C. Grisolia, P.-Y. Thro, In-depth analysis of ITER-like samples composition using laser-induced breakdown spectroscopy, J. Nucl. Mater. 414 (3) (2011) 485–491.
[15] J. Karhunen, A. Hakola, J. Likonen, A. Lissovski, P. Paris, M. Laan, K. Piip, C. Porosnicu, C.P. Lungu, K. Sugiyama, Development of laser-induced breakdown spectroscopy for analyzing deposited layers in ITER, Phys. Scr. T159 (2014) 4.
[16] P. Paris, K. Piip, A. Hakola, M. Laan, M. Aints, S. Koivuranta, J. Likonen, A. Lissovski, M. Mayer, R. Neu, V. Rohde, K. Sugiyama, Development of laser induced breakdown spectroscopy for studying erosion, deposition, and fuel retention in ASDEX Upgrade, Fusion Eng. Des. 98-99 (2015) 1349–1352.
[17] G.S. Maurya, A. Jyotsana, R. Kumar, A. Kumar, A.K. Rai, In situ analysis of impurities deposited on the tokamak flange using laser induced breakdown spectroscopy, J. Nucl. Mater. 444 (1-3) (2014) 23–29.
[18] A. Semerok, C. Grisolia, LIBS for tokamak plasma facing components characterisation: perspectives on in situ tritium cartography, Nucl. Instrum. Methods Phys. Res. Sect. A-Accel. Spectrom. Dect. Assoc. Equip. 720 (2013) 31–35.
[19] G. Counsell, P. Coad, C. Grisola, C. Hopf, W. Jacob, A. Kirschner, A. Kreter, K. Krieger, J. Likonen, V. Philipps, J. Roth, M. Rubel, E. Salancon, A. Semerok, F.L. Tabares, A. Widdowson, J.E. contributors, Tritium retention in next step devices and the requirements for mitigation and removal techniques, Plasma Phys. Control. Fusion 48(12B) (2006) B189-B199.
[20] C. Grisolia, G. Counsell, G. Dinescu, A. Semerok, N. Bekris, P. Coad, C. Hopf, J. Roth, M. Rubel, A. Widdowson, E. Tsitrone, Treatment of ITER plasma facing components: current status and remaining open issues before ITER implementation, Fusion Eng. Des. 82 (15–24) (2007) 2390–2398.
[21] Salvatore Almaviva, Luisa Caneve, Francesco Colao, Giorgio Maddaluno, Deuterium detection and quantification by laser-induced breakdown spectroscopy and calibration-free analysis in ITER relevant samples, Fusion Eng. Des. 146 (2019) 2087–2091.
[22] P. Paris, J. Butikova, M. Laan, M. Aints, A. Hakola, K. Piip, I. Tufail, P. Veis, Detection of deuterium retention by LIBS at different background pressures, Phys. Scr. T170 (2017) 5.
[23] A. Malaquias, V. Philipps, A. Huber, A. Hakola, J. Likonen, J. Kolehmainen, S. Tervakangas, M. Aints, P. Paris, M. Laan, A. Lissovski, S. Almaviva, L. Caneve, F. Colao, G. Maddaluno, M. Kubkowska, P. Gasior, H.J. van der Meiden, A.R. Lof, P. A. Zeijlmans van Emmichoven, P. Petersson, M. Rubel, E. Fortuna, Q. Xiao, Development of ITER relevant laser techniques for deposited layer characterisation and tritium inventory, J. Nucl. Mater. 438 (2013) S936–S939.
[24] P. Gasior, M. Bieda, M. Kubkowska, R. Neu, J. Wolowski, Laser induced breakdown spectroscopy as diagnostics for fuel retention and removal and wall composition in fusion reactors with mixed-material components, Fusion Eng. Des. 86 (6-8) (2011) 1239–1242.
[25] A. Ciucci, M. Corsi, V. Palleschi, S. Rastelli, A. Salvetti, E. Tognoni, New procedure for quantitative elemental analysis by laser-induced plasma spectroscopy, Appl. Spectrosc. 53 (8) (1999) 960–964.
[26] P. Veis, A. Marin-Roldan, J. Kristof, Simultaneous vacuum UV and broadband UV-NIR plasma spectroscopy to improve the LIBS analysis of light elements, Plasma Sources Sci. Technol. 27 (9) (2018) 18.

[27] P. Veis, A. Marín-Roldán, V. Dwivedi, J. Karhunen, P. Paris, C. Jõgi, C.P. Porosnicu, V. Lungu, A. Hakola Nemanic, Quantification of H/D content in Be/W mixtures coatings by CF-LIBS, Phys. Scr. 171 (2020) 7.
[28] M. Suchoňová, J. Krištof, M. Pribula, M. Veis, F.L. Tabarés, P. Veis, Analysis of LiSn alloy at several depths using LIBS, Fusion Eng. Des. 117 (2017) 175–179.
[29] A. Hakola, K. Heinola, K. Mizohata, J. Likonen, C. Lungu, C. Porosnicu, E. Alves, R. Mateus, I.B. Radovic, Z. Siketic, V. Nemanic, M. Kumar, C. Pardanaud, P. Roubin, E.U.W.P. Contributors, Effect of composition and surface characteristics on fuel retention in beryllium-containing co-deposited layers, Phys. Scr. T171 (1) (2020) 8.
[30] A. Kramida, Y. Ralchenko, J. Reader, and NIST ASD Team, *NIST Atomic Spectra Database* (ver. 5.8), [Online]. Available: https://physics.nist.gov/asd. National Institute of Standards and Technology, Gaithersburg, MD. https://doi.org/10.18434/T4W30F.
[31] E. Tognoni, G. Cristoforetti, S. Legnaioli, V. Palleschi, A. Salvetti, M. Mueller, U. Panne, I. Gornushkin, A numerical study of expected accuracy and precision in Calibration-Free Laser-Induced Breakdown Spectroscopy in the assumption of ideal analytical plasma, Spectroc. Acta Pt. B-Atom. Spectr. 62 (12) (2007) 1287–1302.